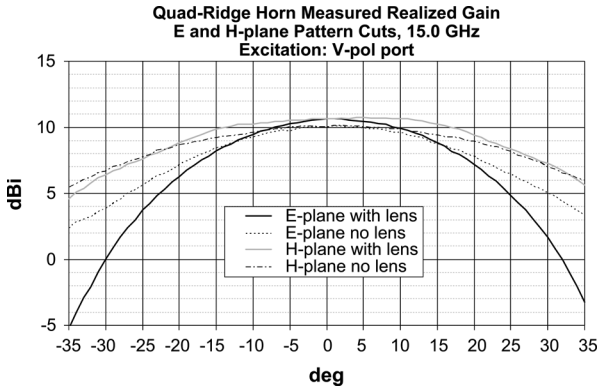

Fig. 10. E and H-plane Pattern cuts, 15 GHz, with and without lens.

receiver with time gating could be used to remove the effects of such reflections on the gain measurement and was not available at the time of this measurement.

Fig. 10 shows E and H-plane pattern cuts with and without the lens. A larger difference in beamwidth between the lens and no lens case can be seen in the E-plane since the lens yields phase correction of the near fields for the E-plane only. The shape of the lens could be optimized to trade boresigth gain for pattern symmetry. If such a requirement was imposed a similar parametric study and design approach could be easily employed.

V. Conclusion

The addition of a light weight dielectric lens to a dual-polarized quad-ridge horn has shown to improve the boresight efficiency over the 5–15 GHz band and achieve 70% aperture efficiency over most of the band. The dielectric lens did not significantly impact the S11 or isolation of either the H-pol or V-pol ports; S11 of less than -10 dB over most of the band was achieved with a worst case of -7.5 dB.

The finite element method has shown to produce results that are in reasonable agreement with all of the measurements including E-plane and H-plane pattern measurements with the exception of: x-pol pattern levels less than approximately -20 dBi and port-port isolation. This is most likely due to manufacturing tolerances not included in the model and noise from the measurement; such noise sources include x-pol from the anechoic chamber source antenna, antenna misalignments, and scattering from floor and the antenna fixtures. However, in general the finite element method has proven to be a very accurate tool that can be used to design or modify existing designs of a quad-ridge horn or a similar type of 3-D radiating structure that includes a dielectric lens.

References

[1] L. De Haro, A. G. Pino, J. L. Besada, A. M. Arias, and J. O. Rubinos, "Antennas feasibility study for a LMDS communication system," in *Proc. Antennas and Propag. Society Int. Symp.*, Jul. 11–16, 1999, vol. 3, pp. 2162–2165.

[2] R. Peritz, "A matched dielectric lens in a highly flared horn to produce focused feed patterns for a cassegrain antenna," in *Proc. Antennas and Propag. Society Int. Symp.*, Sep. 1964, vol. 2, pp. 196–202.

[3] A. D. Olver and B. Philips, "Integrated lens with dielectric horn antenna," *Electron. Lett.*, vol. 29, no. 13, pp. 1150–1152, Jun. 1993.

[4] R. O. dos Santos and C. L. S. S. Sobrinho, "FDTD method: Analysis of an one-dimensional array of H-plane sectoral horn antennas with dielectric lens," in *Proc. Microw. Optoelectron. Conf.*, Aug. 6–10, 2001, vol. 1, pp. 481–484.

[5] A. Kezuka, Y. Yamada, and Y. Kazama, "Design of a feed horn for a FWA base station antenna through FDTD method," in *Proc. Joint Conf. 10th Asia-Pacific Conf. on Commun.*, Sep. 1, 2004, vol. 2, pp. 573–576.

[6] L. Oh, S. Peng, and C. Lunden, "Effects of dielectrics on the radiation patterns of an electromagnetic horn," *IEEE Trans. Antennas Propag.*, vol. 18, pp. 553–556, Jul. 1970.

[7] Z. Shen and C. Feng, "A new dual-polarized broadband horn antenna," *IEEE Antennas Wireless Propag. Lett.*, vol. 4, pp. 270–273, 2005.

[8] S. Soroka, "A physically compact quad ridge horn design," in *Proc. Antennas and Propag. Society Int. Symp.*, Jun. 1986, vol. 24, pp. 903–906.

[9] M. Botello-Pérez, H. Jardón-Aguilar, and I. García Ruíz, "Design and simulation of a 1 to 14 GHz broadband electromagnetic compatibility DRGH antenna," in *Proc. 2nd Int. Conf. on Elect. and Electron. Engineer.*, Sep. 7–9, 2005, pp. 118–121.

[10] H. Lai, R. Franks, D. Kong, D. Kuck, and T. Gackstetter, "A broad band high efficent quad ridged horn," in *Proc. Antennas and Propag. Society Int. Symp.*, Jun. 1987, vol. 25, pp. 676–679.

[11] A. D. Olver, P. J. B. Clarricoats, A. A. Kishk, and L. Shafai, *Microwave Horns and Feeds*. New York: IEEE Press, 1994, pp. 370–390.

Dual-Ring Circularly-Polarized Microstrip Patch Array Using Hybrid Feed

Chunwei Min and Charles E. Free

***Abstract*—We describe the design of a new form of traveling-wave-fed, circularly polarized microstrip patch array at X-band. The antenna employs a dual-ring array structure in which the radiating elements are fed by non-radiating slots with sequential phase excitations to generate circular polarization. The antenna incorporates two novel features: firstly, two concentric ring sub-arrays of linearly polarized elements are used to improve the axial ratio and, secondly, development of a new model for power distribution to ensure that all the elements radiate the same power, thus ensuring pattern symmetry and high-quality circular polarization. The proposed design was validated through practical measurements, which showed a well-matched antenna with good axial ratio and well-defined radiation patterns.**

***Index Terms*—Aperture-coupled, circular arrays, circular polarization, hybrid feed, microstrip antennas.**

I. Introduction

The operation of circularly polarized (CP) microstrip antennas may be viewed as the superposition of two or more linearly polarized (LP) modes with equal amplitudes and appropriate phasing to generate a rotating field. Various techniques for generating CP waves have been reported in the literatures. The antenna can utilize LP or CP element, and can be fed using various feed mechanisms. Typical feed structures are: an offset feed to a single patch; two feeds with phase quadrature; sequential feed to a multi-element array. Huang [1] first proposed the use of four LP patches, positioned orthogonally, and fed sequentially with 90° phase shifts. A wideband square microstrip patch antenna was proposed in [2], using a corporate feed network with sequential phase-shifts for CP operation. In [4], a patch antenna array using CP elements and sequential rotation via a serial feed arrangement was presented.

Manuscript received April 11, 2008; revised June 25, 2008. Current version published June 03, 2009.

The authors are with the Advanced Technology Institute, Faculty of Engineering and Physical Sciences, University of Surrey, Guildford Surrey GU2 7XH, U.K. (e-mail: C.Min@surrey.ac.uk).

Digital Object Identifier 10.1109/TAP.2009.2019984

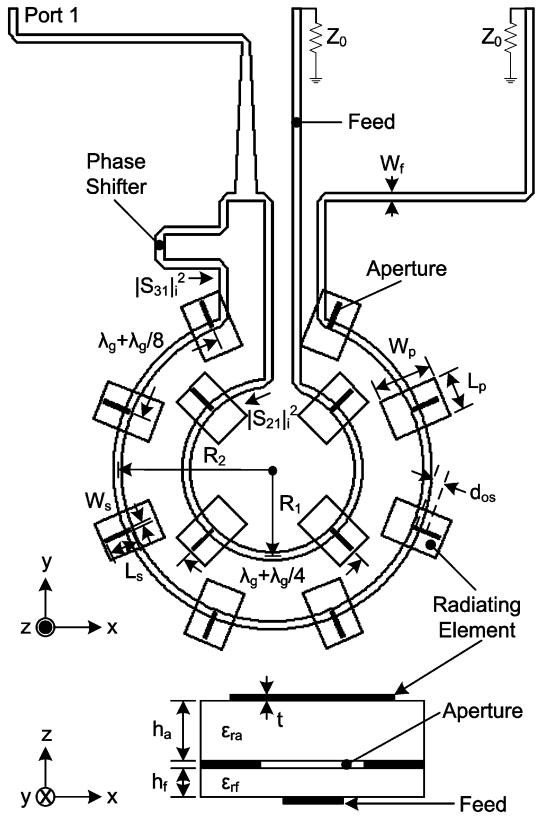

Fig. 1. Configuration of the proposed antenna.

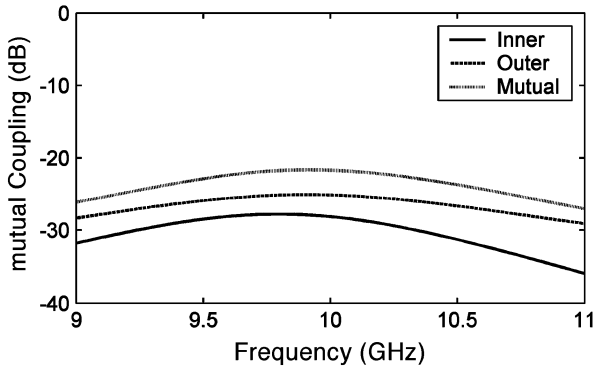

Fig. 2. Simulated mutual coupling levels between adjacent elements.

An axial ratio bandwidth $(\mathrm{ARBW} < 3\ \mathrm{dB})$ of 3.5% was obtained in this latter work. A serial feed with sequential phase shift underneath a square patch coupled by a cross slot for CP was proposed in [5]. This technique simplified the feed network on single element, and a 4.6% ARBW was reported. Using the basic principle from Min and Free [6] showed that the patches could be arranged in an annular configuration to achieve good CP quality.

The work described in this paper extends the techniques previously reported in the literatures to provide a microstrip CP antenna with enhanced radiation properties. A novel arrangement of dual concentric ring arrays, shown in Fig. 1, is fed by a hybrid feed network such that the phase distribution to the patches will generate CP waves. The primarily benefit of the new arrangement is that there is a more uniform distribution of radiating elements, compared to previously reported designs, and this should enhance the quality of CP radiation.

However, a critical requirement for this type of antenna is that all the radiating elements should radiate the same amount of power. Clearly, with a sequential feed technique, some scheme is necessary for successively changing the amount of energy coupled to each patch. This issue has largely been ignored by previous authors. Therefore, a schematic model was developed so that each radiating element will receive an identical amount of power from the feed line. The required coupling was achieved using non-resonant slots in the ground plane beneath each patch, as shown in Fig. 1, these slots being fed from a microstrip line on the side of the antenna. Measured results are presented to confirm the validity of the design and proposed model for power feeding.

II. Model for Coupled Power Control

The configuration of the proposed traveling-wave (TW)-fed, dual-ring array is shown in Fig. 1. The microstrip feed line is formed on one side of the circuit and the radiating elements on the other. The microstrip and radiating elements share a common ground plane that contains apertures to couple power from the microstrip line to the patches. The aperture-coupled feed technique was first proposed by Pozar [3] in which a non-resonant aperture slot was utilized for the excitation of radiating elements. This technique can conveniently be applied on a TW feed line. The propagating fields along the feed line induce a magnetic current along the aperture slot, and a portion of energy is coupled to the radiating element at resonance. Since power is coupled out through each slot in turn, leaving less for the remaining slots and patches, increased coupling is required for patches excited further down the line. The coupling is adjusted by offsetting the slots from the center of the line by a distance (d_{os}), as shown in Fig. 1. This concept provides design flexibility to guarantee that each radiating element is able to receive an identical amount of power from the feed line. It was found that a larger offset of the slot resulted in less power being coupled to the patch.

Fig. 2 shows the simulated mutual coupling levels between adjacent elements in the array. They were found to be all below -20 dB, which were relatively small, and may have negligible effects back to the structure. This condition enabled to analyze and formulate the coupling behaviors within the array. The proposed model for coupled power control is shown in Fig. 3. It is seen that the input power is split between the inner and outer rings. Since the radiating elements were connected in cascade and fed in a sequential manner, it was important to include in the model the loss factors (L_4 and L_8) in the feed lines between adjacent elements, to ensure that each element received the same amount of power that can be expressed in terms of a power ratio (P_{raN}) relative to the input power (P_{in}). The power delivered to the first element each of the two rings was defined as $|S_{21}|_i^2$ and $|S_{31}|_i^2$, relative to the input power, respectively. The design equations were then derived from various senses of signal propagations within the structure. It was realized that the power delivered to each element had the contributions from the direct power transmission, the reflections from subsequent and preceding elements, and multiple reflections between the elements in the subarrays. It was found that larger delivered power to the elements results in the increase of efficiency. However, larger coupling generates more inductive reactance that causes impedance mismatch around the design's center frequency. Therefore, in order to maintain acceptable reflection level $(|S_{11}|^2 < -10\ \mathrm{dB})$, it is suggested that one may select a coupling factor to be less than 20% of the input power for the terminal elements. Since the direct power transmission from the input dominates the delivered power, and based on the suggested design criterion, the coupling factor (k_c) for each element in the subarrays can then be approximated in terms of the coupled power ratio (P_{raN}) and the propagation behaviors in the structure, as expressed in (1)–(4). One

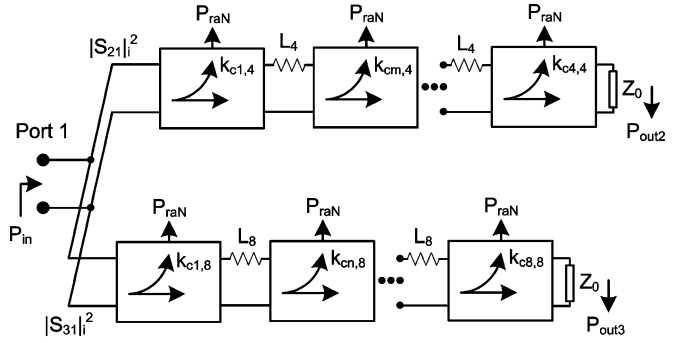

Fig. 3. Model for coupled power control of the dual-ring array.

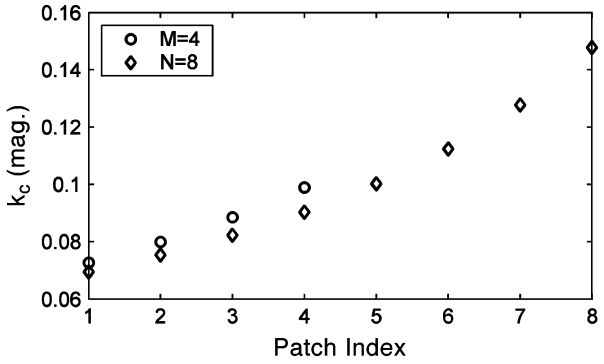

Fig. 4. Coupling (k_c) required from input power of the radiating elements.

may proceed to select an appropriate value of the portion of power delivered to the element, work out the input power for the rings, and deduce the required coupling factor for each element. Full-wave analysis can then be applied to obtain the offset distances needed corresponding to the designed coupling factors of each element from its S-parameters responses using (5). In the proposed antenna design, the parameters were initially selected and summarized as follows: $P_{raN} = 0.03$, $|S_{21}|_i^2 = 0.413$, $|S_{31}|_i^2 = 0.432$, $L_4 = 0.019$, and $L_8 = 0.009$. The calculated results of the coupling factors are shown in Fig. 4. It is obviously seen that the successive elements need more coupled power from the feed channel to maintain identical delivered power. This model can be applied on various non-resonant types of series-fed arrays as long as the coupling mechanism is formed

$$k_{c1,4} \approx \frac{P_{raN}}{|S_{21}|_i^2} \tag{1}$$

$$k_{cm,4} \approx \frac{P_{raN}}{|S_{21}|_i^2 (1-L_4)^{m-1} \prod_{a=1}^{m-1} (1-k_{ca,4})}$$

$$\text{for } m = 2 \text{ to } M, \tag{2}$$

$$k_{c1,8} \approx \frac{P_{raN}}{|S_{31}|_i^2} \tag{3}$$

$$k_{cn,8} \approx \frac{P_{raN}}{|S_{31}|_i^2 (1-L_8)^{n-1} \prod_{b=1}^{n-1} (1-k_{cb,8})}$$

$$\text{for } n = 2 \text{ to } N. \tag{4}$$

$$k_c = 1 - \frac{|S_{21}|^2}{1-|S_{11}|^2}. \tag{5}$$

III. Measurements and Discussion

The radiating patches were arranged in dual circular arrays with appropriate phase delays in the feed between adjacent to produce CP waves. A phase shifter was used prior to the elements to achieve co-phasal patterns, as shown in Fig. 1. The proposed antenna was fabricated using RT/duroid 5880 for both the layers containing the patches, and for the feed network; the measured parameters of the material were $\varepsilon_{ra} = \varepsilon_{rf} = 2.195$, $h_a = 1.575$ mm, $h_f = 0.508$ mm, $t = 0.017$ mm, and $\tan\delta = 0.0014$. Using these materials information, the physical dimensions of the antenna system were obtained as $W_p = 11.9$ mm, $L_p = 8.1$ mm, $W_s = 0.5$ mm, $L_s = 5.4$ mm, and $W_f = 1.6$ mm. The ring radii were selected as $R_1 = 17.3$ mm, and $R_2 = 31$ mm for the $M = 4$ and $N = 8$ subarrays, respectively. Based on the material parameters, the required offset distances were obtained using full-wave analysis, and the results are shown in Fig. 5.

Fig. 6 shows the reflection coefficient ($|S_{11}|$) of the antenna. It can be seen that in general there is good agreement between the simulated and measured results. A transmission/reflection (T/R) efficiency ($e_{T/R}$) was defined as the ratio of the total power consumed in the antenna system to the input power, as shown in Fig. 7. It is obvious that

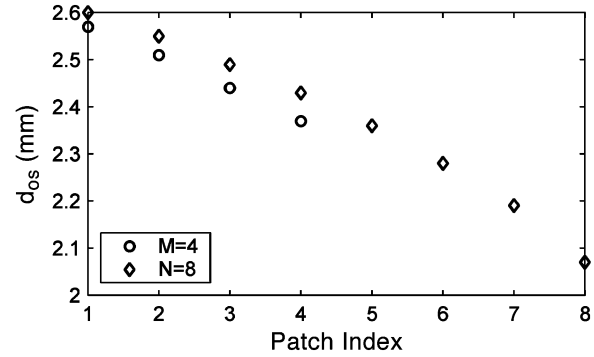

Fig. 5. Offset distances (d_{os}) of the apertures beneath the radiating elements.

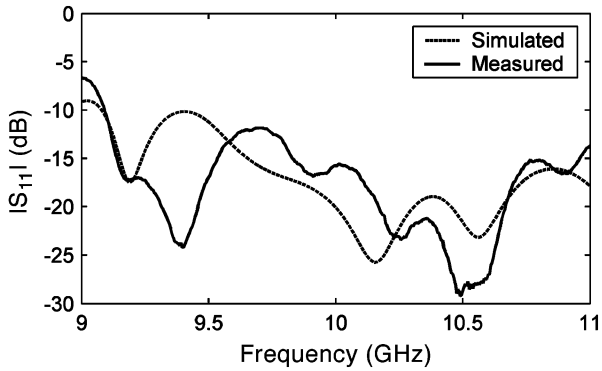

Fig. 6. Reflection coefficient ($|S_{11}|$) of the antenna.

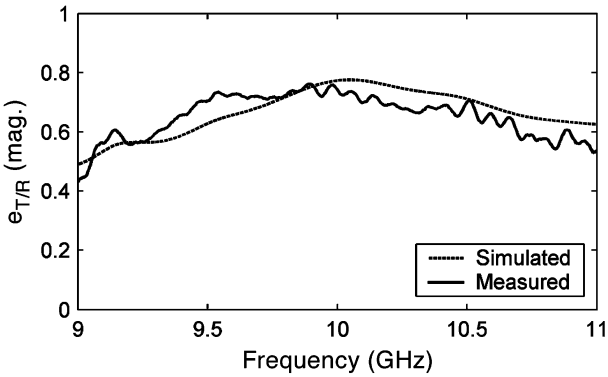

Fig. 7. T/R efficiency ($e_{T/R}$) of the antenna.

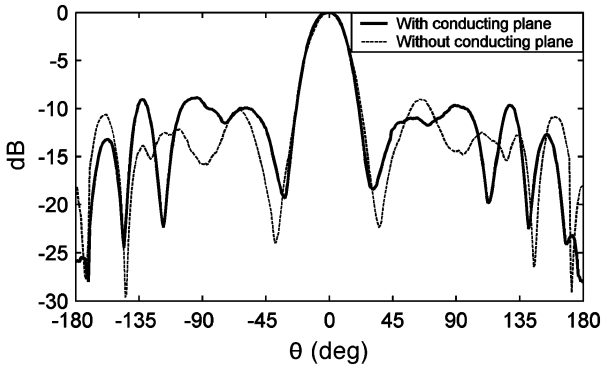

Fig. 8. Measured radiation patterns of the antenna with and without the conducting plane at 10 GHz.

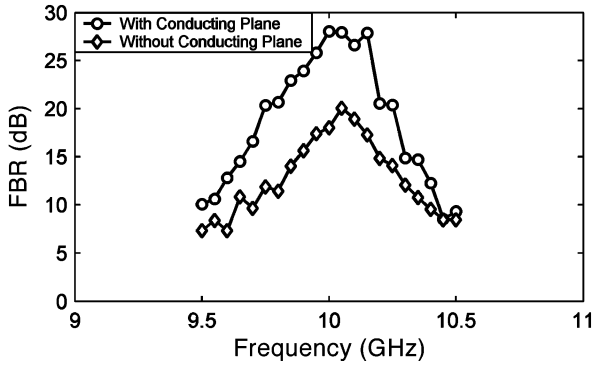

Fig. 9. Measured front-to-back ratio (FBR) of the antenna with and without the conducting plane.

for this type of antenna, one would expect a higher transmission loss through the rings so that little power was wasted in the terminations. It is important to realize that the power consumed in the antenna will be the sum of that radiated, plus that dissipated as loss within the materials of the antenna. By appropriate choices of materials for the antenna, the power lost can be minimized.

Fig. 8 shows the radiation patterns of the antenna at 10 GHz. The patterns were found to be symmetric in the boresight, which means that each radiating element in the array contributes identical amount of power. An additional conducting plane with a size of $4\lambda_0 \times 4\lambda_0$ was placed behind the antenna by a distance of $\lambda_0/4$ away behind the antenna to investigate the pattern characteristics. The first-null beamwidth was narrowed from 70.2° to 61.2° with the conducting plane. Meanwhile, a 10 dB improvement on the front-to-back ratio (FBR) was achieved at the design's center frequency. It is seen from Fig. 9 that the FBR decreased considerably away from the center frequency. It is explained as a fact that the elements contributed less radiation to the boresight due to the decrease of radiation efficiency.

The antenna was formed from a multilayer structure, and it was realized that misalignment errors could have a significant effect on the results. This alignment error will become critical at mm-wave frequencies, and it is suggested that the misalignment should be kept within ±5% of the designed values. The gain of the test antenna can be extracted by measuring the power transmission of the two-antenna system, and compensating for the known losses of the system components. The results are shown in Fig. 10.

Two single-ring arrays with four ($R = 17.3$ mm) and eight ($R = 31$ mm) elements were developed utilizing the proposed design criteria and model for the comparisons of the CP quality with the dual-ring

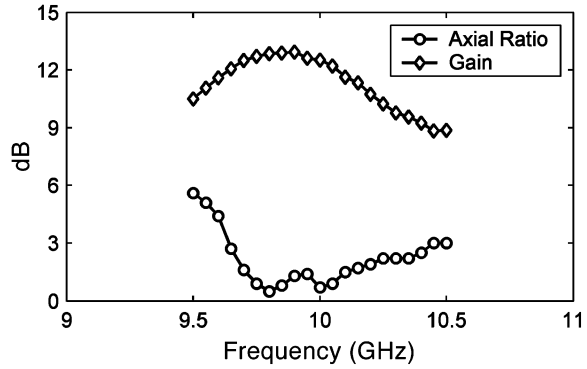

Fig. 10. Measured axial ratio and gain of the antenna.

array design. For the single-ring, four-element array, the best AR was found to be 0.6 dB at 10.05 GHz. The measured ARBW was 7.2%. Good CP quality was also achieved on the eight-element array. The minimal AR was 0.8 dB at 10.1 GHz, and ARBW to be 6.6%. Improved ARBW was found on the dual-ring array with the minimal AR of 0.5 dB at 9.8 GHz and ARBW of 8.5%. The symmetry of measured radiation patterns in conjunction with good CP quality achieved have proven the proposed model for power control to be valid and applicable for the series-fed CP array designs.

IV. Conclusion

The design of a novel TW-fed CP antenna has been established through practical measurements. The measured results were in good agreement with those predicted from theoretical simulations. The measured antenna exhibited good CP quality at the design frequency, with well-behaved radiation patterns and moderately high gain. Due to the trade-off between the system efficiency and reflection levels in the antenna, one may improve the efficiency by selecting a larger value for the delivered power to the elements with the inclusions of the reflections in the antenna. The proposed model can then be further expanded to improve the performance of the antenna whilst maintaining CP quality. This type of antenna has good potential for further development, both as a wideband antenna, and also for inclusion in planar microwave integrated circuits.

References

[1] J. Huang, "A technique for an array to generate circular polarization with linearly polarized elements," *IEEE Trans. Antennas Propag.*, vol. AP-34, no. 9, pp. 1113–1123, Sep. 1986.

[2] S. D. Targonski and D. M. Pozar, "Design of wideband circularly polarized aperture-coupled microstrip antennas," *IEEE Trans. Antennas Propag.*, vol. 41, no. 2, pp. 214–220, Feb. 1993.

[3] D. M. Pozar, "A microstrip antenna aperture coupled to a microstripline," *Electron. Lett.*, vol. 21, pp. 49–50, Jan. 1985.

[4] H. Evans, P. Gale, B. Aljibouri, E. G. Lim, E. Korolkeiwiez, and A. Sambell, "Application of simulated annealing to design of serial feed sequentially rotated 2 × 2 antenna array," *Electron. Lett.*, vol. 36, no. 24, pp. 1987–1988, Nov. 2000.

[5] H. Kim, B. M. Lee, and Y. J. Yoon, "A single-feeding circularly polarized microstrip antenna with the effect of hybrid feeding," *IEEE Antennas Wireless Propag. Lett.*, vol. 2, pp. 74–77, 2003.

[6] C. Min and C. E. Free, "Design of a traveling-wave aperture-coupled circularly-polarized concentric ring array," in *Proc. 37th Eur. Microw. Conf.*, Munich, Germany, Oct. 2007, pp. 1519–1522.